Supplemental Materials

S.1. Combustor model

The combustor operation is modeled by solving the following equations between the *inlet* and *exit* states:

Mass: $\dot{m}_{inlet} = \dot{m}_{exit}$ where $\dot{m} = \rho v$, ρ is the density and v is the velocity of the gas.

Momentum: $(P + \rho v^2)_{inlet} = (P + \rho v^2)_{exit}$, where P is the pressure

Energy: $(h + 0.5v^2)_{inlet} = (h + 0.5v^2)_{exit}$, where h is the total enthalpy per unit mass, including chemical and thermal forms.

At the inlet, temperature (T), P, composition (through model fractions, X_i) and v are specified. At the exit, chemical equilibrium is enforced (using Cantera), subject to the constraints of mass, momentum, and energy conservation, as expressed by the abovementioned equations. Only one set of T, P, v, and X_i at the exit will satisfy these constraints. For subsonic inlet conditions, valid solutions are obtained when the exit velocity is also subsonic or the flow is not choked.

S.2. MgO-Atmosphere Interaction Thermodynamics and Kinetics

As mentioned in the main body, a cooperative adsorption-diffusion-dissolution mechanism is proposed in which water and CO_2 adsorb onto an MgO particle forming a solution containing Mg^{2+}, OH^-, H^+, CO_3^{2-}, HCO_3^- and CO_2. Assuming adsorption, diffusion in liquid water, and MgO dissolution are relatively fast (see below), the solution is in equilibrium with the atmosphere, with equilibrium constants [1]:

- $[H^+][OH^-] = K_{aq} = 10^{-14}$ mol^2/l^2
- $[H^+][CO_3^{2-}] \div [HCO_3^-] = K_{HCO_3} = 4.96\times10^{-11}$ mol/l
- $[H^+][HCO_3^-] \div [CO_2] = K_{HHCO_3} = 4.27\times10^{-7}$ mol/l
- $[CO_2] \div pCO_2 = K_{CO_2} = 3.80\times10^{-5}$ mol/(l·Pa)

Assuming droplet charge neutrality gives:

$$2[Mg^{2+}] + [H^+] - [OH^-] - [HCO_3^-] - 2[CO_3^{2-}] = 0 \quad \text{(S.1)}$$

Setting $X = [HCO_3^-]$ and substituting the above equilibrium conditions gives:

$$-2KHCO_3KHHCO_3[CO2]\ X3\text{-}KaqKHHCO_3[CO2]+1X2+2[Mg^{2+}]X+KHHCO_3[CO2]=0 \quad \text{(S.2)}$$

The included spreadsheet solves this equation, and Fig. S.1 below shows total carbon concentration, including dissolved CO_2, CO_3^{2-} and HCO_3^-, as well as the "excess" C:Mg mole ratio (subtracting total carbon when $[Mg^{2+}]=0$) for p_{CO_2} = 40 Pascals. This calculation shows that at high magnesium concentration, for relatively small droplets, a droplet at equilibrium has twice as many moles of excess carbon as magnesium, essentially as dissolved $Mg(HCO_3)_2$; in the limit of low magnesium concentration, i.e. for relatively large droplets, a droplet has as many moles of excess carbon as magnesium, essentially as dissolved $MgCO_3$. Thus, if these droplets are at equilibrium with the atmosphere, each mole of MgH_2 fuel burned will likely absorb at least one mole of CO_2 from the atmosphere.

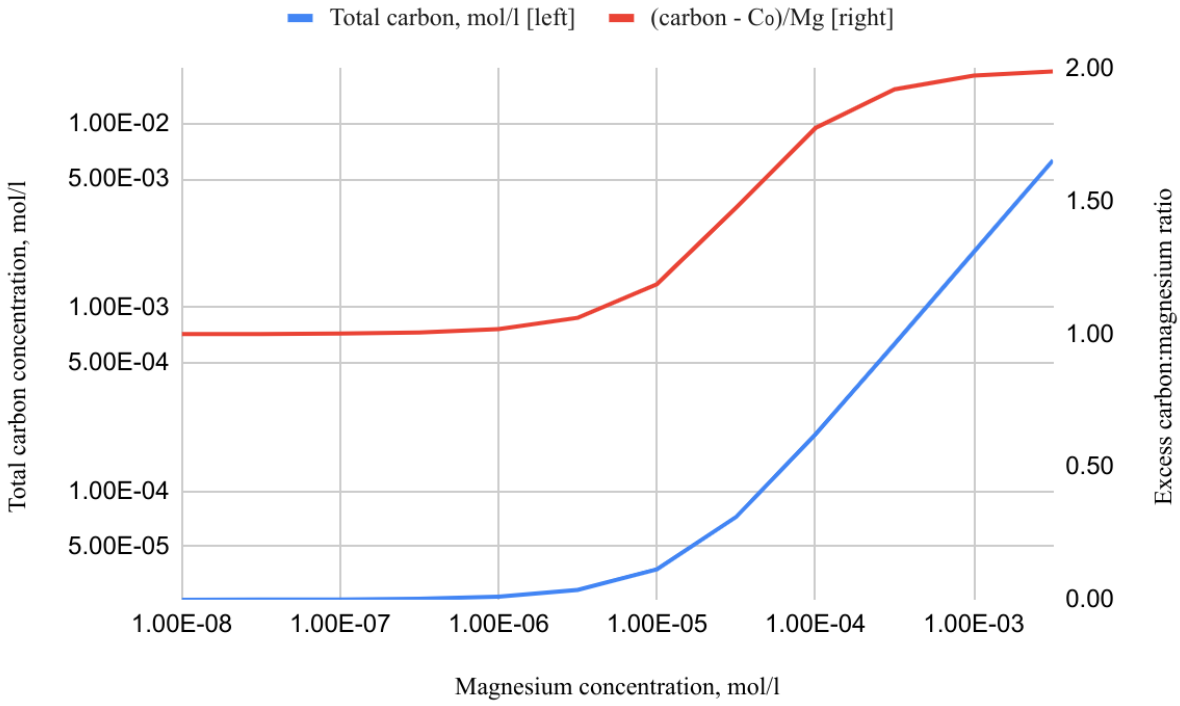

In terms of kinetics, the Langmuir adsorption equation describes the CO_2 collision rate:

$$JCO2=pCO22MCO2RT \quad (S.3)$$

Here, p_{CO2} is the CO_2 partial atmospheric pressure at an assumed cruising altitude of 10 kilometers (approximately 10 Pa), T is the standard atmospheric temperature at that altitude (approximately 223.25 K),

M_{CO2} carbon dioxide's molar mass, and R the universal gas constant. This gives a molar CO_2 flux J_{CO2} of 0.4492 moles/m²·s. In order to find the theoretical growth rate of an outer carbonate layer in and around each MgO exhaust particle, the CO_2 flux is multiplied by the molar mass of $MgCO_3$ and divided by the carbonate's density. This gives a rate of 12.9 microns per second. This can be considered an upper limit to the growth rate of the carbonate as the reaction proceeds, i.e. a limit to how fast carbonation can occur based on how quickly CO_2 can possibly be incident upon a hypothetical MgO surface.

Since the length scale of this growth rate is much greater than the diameter of an MgH_2 or MgO particle, CO_2 adsorption does not limit carbonate growth rate on exhaust particles. More broadly, carbonation kinetics of fine or porous MgO do not depend on total or partial pressure over a wide range of conditions [2], which determines the CO_2 concentration and would thus influence this growth rate limit. Other factors must limit the rate and/or degree of carbonation. In fact, the kinetics of solid MgO carbonation are slow, even in the presence of moisture. There is strong evidence proving the formation of the aforementioned $MgCO_3$ "shell," and that this acts as a diffusion barrier hindering further CO_2 absorption [3, 4].

Diffusivity of Mg^{2+} in liquid water is about 10^{-5} cm^2/s [5], so a 1 mm droplet with negligible convection takes ~10^3 seconds to equilibrate. The one other potential limiting mechanism is MgO reaction with and dissolution into liquid water, whose kinetics are unknown to the authors.

The settling of particles in the atmosphere occurs by diffusion for small particles, and at gravitational terminal velocity for large particles. The maximum residence time for a particle with radius between approximately 10^{-2} and 10 microns in the tropopause (which includes the assumed cruising altitude) is between 1 and 100 days, depending on the settling mechanism [6]. Since CO_2 absorption itself can be considered fast and a water droplet reaches diffusive equilibrium in ~10^3 seconds, when the MgO reaches the earth's surface, it will be in equilibrium with CO_2 and water vapor in the lower atmosphere. Though the individual solubilities of MgO (as $Mg(OH)_2$) and CO_2 (as H_2CO_3) are relatively small due to their basicity and acidity, respectively, the process of cooperative MgO dissolution as well as water and CO_2 absorption with interdiffusion described above should create $Mg(HCO_3)_2$ and/or $MgCO_3$ solution droplets with close to

neutral pH. And as long as MgO dissolution is not excessively slow, this should happen relatively quickly (compared with settling times). Thus, it can be reasonably stated that all carbonate droplets will return to the very moist lower atmosphere in timescales shorter than needed for the intended climate amelioration effect.

S.2. MgH_2 Production GHG Emissions

As described above, the emissions of "gray", "blue" (both from natural gas) and "green" (water electrolysis) hydrogen production are well known, and green hydrogen has good prospects for cost reduction in the coming years [7, 8]. And it is straightforward to produce MgH_2 from Mg and H_2 [9]. But magnesium production emissions are high, from 2.5-42 kg CO_2e/kg Mg, depending on the process, which is much higher than the 1.8-3.6 kg CO_2 removed per kg Mg burned. We consider here what kinds of magnesium production processes would result in supply chain CO_2-equivalent emissions below the amount of CO_2 removed by aviation combustion.

The most important emissions determinant is magnesium compound reduction technology, with two dominant process categories. Thermal processes such as Balzano, Magnatherm and Pidgeon use ferrosilicon reduction at low pressure with a temperature gradient following the reaction: $2\ MgO + Si \rightarrow SiO_2 + Mg$. These use about 430-570 MJ energy/kg Mg, and emit 10-42 kg CO_2e/kg Mg mostly due to fossil energy consumption for heating. [10] , with most in the range of 20-27 [11, 12]. Electrolytic processes reduce anhydrous $MgCl_2$ to magnesium metal at 680-760°C, with a chlorine gas by-product, and no direct GHG emissions, though $MgCl_2$ dehydration requires HCl vapor atmosphere, making it expensive, and it currently uses fossil fuel thermal energy. [13] This flowsheet results in 5-7 kg CO_2e/kg Mg [11, 12, 14]. A variation on this at Alliance Magnesium in Quebec uses hydrogen in a porous anode to produce the anhydrous HCl used in drying; this flow sheet emits just 2.5 kg CO_2e/kg Mg [15]. Another option is MgO molten salt electrolysis with a reactive metal cathode, such as tin or lead, followed by distillation to recover Mg [16, 17, 18, 19], with a carbon anode this emits 0.9-1.8 kg CO_2 per kg Mg, and inert anodes with no direct emissions in operation are in their infancy [19, 20, 21, 22].

Extraction from brines of anhydrous $MgCl_2$ and MgO for electrolysis generally follows one of three processes:

- Drying and calcining $Mg(OH)_2$ to MgO is usually done by fossil fuel heating, though in principle it can be done with electric heating e.g. resistance, with ultrasonic or direct solar drying as more efficient options.
- Dry MgO can be converted to anhydrous $MgCl_2$ via carbochlorination following the reaction $2\ MgO + Cl_2 + C \rightarrow MgCl_2 + CO_2$, though 1.8 kg CO_2 emissions per kg Mg would rule this out.
- Addition of HCl to $Mg(OH)_2$ suspension makes a pure $MgCl_2$ solution, which can be dried by heating in HCl vapor; this drying operation requires vessels made of costly corrosion-resistant alloys.

Raw material is assumed to be precipitated $Mg(OH)_2$ from brines or seawater, rather than $MgCO_3$ from mined rock, as using the latter would result in direct CO_2 emissions. $Mg(OH)_2$ precipitation threshold pH is considerably lower than those of NaOH, $Ca(OH)_2$, KOH and many others, so adding a base to brines, seawater, or seawater concentrate separates out the magnesium. Industrial operations typically use slaked lime $Ca(OH)_2$, dolime $Ca(OH)_2 \cdot Mg(OH)_2$, or caustic soda NaOH. Because the first two generally come from calcined limestone $CaCO_3$ or dolomite $CaCO_3 \cdot MgCO_3$ with direct CO_2 emission, we omit those here, and focus on NaOH. Indeed, the large Dow Chemical magnesium operation in Freeport, Texas which produced most of the world's magnesium from about 1940-1990 was able to use either concentrated NaOH solution co-product of chlorine production made by the chlor-alkali process, or slaked lime or dolime. Zero-direct-emissions magnesium production should thus begin with chlor-alkali production of NaOH, and proceed with one of the two options described above as shown in Figure S.2. Note the *X* indicates excess NaOH required to raise pH and begin to precipitate $Mg(OH)_2$, that ratio varies by $MgCl_2$ source. With option ①, hydrogen and chlorine from the chlor-alkali process can provide HCl needed for anhydrous $MgCl_2$ production; with option ② the hydrogen is available for making MgH_2. Both produce chlorine gas as a by-product. The net reactions for options ① and ② are thus:

① $MgCl_2 \rightarrow Mg + Cl_2$ (S.4)

② $MgCl_2 + H_2O \rightarrow Mg + Cl_2 + H_2 + ½O_2$ (S.5)

Either way, including hydride production or water hydrolysis, and the aircraft wake/atmosphere reaction between MgO and CO_2, the overall net reaction is:

$MgCl_2 + ½O_2 + CO_2 \rightarrow MgCO_3 + Cl_2$ (S.6)

Essentially, $MgCl_2$ in the oceans is replaced with $MgCO_3$. This slightly increases pH, and increases the CO_2 carrying capacity of the oceans. Note however that if the chlorine returns to the oceans as HCl, this could decrease pH enough to re-release CO_2 back into the atmosphere, or prevent its later absorption. This sector will be a minuscule participant in overall atmosphere-ocean chemistry, but it's important to understand the net effect of using this fuel.

Figure S.2: Magnesium metal production options without direct CO_2 emissions: ① conventional chloride electrolysis, ② oxide electrolysis with inert anode.

Global jet fuel consumption in 2019 totaled 363 billion liters, i.e. 305 Mt. Providing equivalent range would require about 1.32 times as much 65% slurry i.e. 400 Mt, of which 65% or 260 Mt is MgH_2 and 240 Mt of that is Mg. Current world desalination plants consume about 86 Gt/a sea water and produce 35 Gt/a fresh water, with concentrate containing about 110 Mt/a Mg. [23] This is just under half of the 240 Mt/a Mg required to satisfy 2019 aviation fuel consumption. Note there is a potential synergy between desalination and Mg production: an increase in demand for Mg could provide an incentive to build combined desalination+Mg facilities.

In addition, producing 240 Mt/a from sea water or brine would involve production of just over 700 Mt/a of Cl_2, which is much larger than the 87 Mt/a produced worldwide today. Though not quite this simple, it is clear that large-scale magnesium production must be accompanied by large-scale chlorine use in order to achieve effective sequestration.

S.3. Comparisons with Other Fuels

The relevant comparison is between 100% hydrocarbons and a hydrocarbon-MgH_2 slurry. Here we will use just 65% slurry for comparison, replacing 1 t fossil fuel with 1.32 t slurry of which 858 kg MgH_2 containing 792 kg Mg replaces 462 kg fuel. As dodecane, combustion of the fuel would emit 1.43 t CO_2, and the 1:1 C:Mg ratio in 65/35 slurry means combustion of 858 kg MgH_2 absorbs the same 1.43 t CO_2.

To compare with fossil fuels, multiply the 1.43 t in direct emissions by 1.3 to account for upstream emissions in drilling, refining and transportation, leading to 1.87 t CO_2e. Because MgH_2 absorbs 1.43 t CO_2, the replacement reduces combustion and fossil fuel production emissions by 3.29 t. Production of 792 kg Mg to replace 1 t of fossil jet fuel can therefore emit 4.15 kg CO_2e/kg Mg for parity. To the authors' knowledge, Alliance Magnesium is the one producer in the world below this threshold today [15].

Biofuels and synthetic fuel from CO_2 direct air capture (DAC) are more complex. Biofuels have many feedstocks, and many paths to aviation fuel, as described in comprehensive reviews such as [24]. DAC can take many forms based on organic or inorganic media. Both can be at best net-zero GHG emissions, in that case the MgH_2 absorption post-combustion of 1.43 t CO_2 from 792 kg Mg implies that magnesium production emissions for GHG parity would be 1.81 t CO_2e/t Mg. Conversely, if magnesium is produced using the Alliance process with 2.5 t CO_2e/t Mg emissions, then at overall emissions parity, biofuel or synthetic fuel production emissions would be 1.19 t CO_2e/t hydrocarbon.

Energy comparisons are less straightforward. An energy use estimate of CO_2 Direct Air Capture (DAC) by Keith is 280 kJ/mol [Keith 6.36 GJ/t CO_2], theoretical energy to produce dodecane is 660 kJ/mol C, at 50% efficiency that's 1320 kJ/mol C, +280 = 1600 kJ/mol, delivering 660 kJ/mol of oxidation enthalpy, so efficiency is 41%. By comparison, magnesium production efficiency is about 50%, making it slightly more efficient as an electrofuel.

In summary, if the magnesium production process maintains its rough 50% efficiency (as enthalpy of oxidation divided by total energy input for its production), and its emissions can fall below 1.81 t CO_2e/t Mg plus emissions associated with biofuel or synthetic fuel by DAC, then MgH_2 slurry substitution will

result in unconditionally lower net emissions and lower energy use. But as noted above, the required magnesium production scale is orders of magnitude higher than today's ~1Mt/a.

Supplemental Material References

1. Shapley. (n.d.). Dissolved Oxygen and Carbon Dioxide. Chemistry 102 index. Retrieved 2020, from http://butane.chem.uiuc.edu/pshapley/GenChem1
2. G. Song, X. Zhu, R. Chen, Q. Liao, Y.-D. Ding, and L. Chen, "An investigation of CO2 adsorption kinetics on porous magnesium oxide," *Chemical Engineering Journal*, 283, 175–183, Jan. 2016, doi: 10.1016/j.cej.2015.07.055.
3. S. Kumar and S. K. Saxena, "A comparative study of CO2 sorption properties for different oxides," *Mater Renew Sustain Energy,* 3(3), 30, Sep. 2014, doi: 10.1007/s40243-014-0030-9.
4. S. Kumar, S. K. Saxena, V. Drozd, and A. Durygin, "An experimental investigation of mesoporous MgO as a potential pre-combustion CO2 sorbent," *Mater Renew Sustain Energy*, 4(2), 8, Jun. 2015, doi: 10.1007/s40243-015-0050-0.
5. Miller, D. G., Rard, J. A., Eppstein, L. B., & Albright, J. G. (1984). Mutual diffusion coefficients and ionic transport coefficients lij of magnesium chloride-water at 25.degree.C. *The Journal of Physical Chemistry*, 88(23), 5739–5748. https://doi.org/10.1021/j150667a056
6. C. Anastasio and S. T. Martin, "Atmospheric Nanoparticles," *Reviews in Mineralogy and Geochemistry*, 44(1), 293–349, Jan. 2001, doi: 10.2138/rmg.2001.44.08.
7. Schmidt, O., Melchior, S., Hawkes, A., & Staffell, I. (2019). Projecting the Future Levelized Cost of Electricity Storage Technologies. *Joule*, 3(1), 81–100. https://doi.org/10.1016/j.joule.2018.12.008
8. Howarth, R. W., & Jacobson, M. Z. (2021). How green is blue hydrogen? *Energy Science & Engineering*, 9(10), 1676–1687. https://doi.org/10.1002/ese3.956
9. Brown, K. S., Jr., Bowen, D. D. G., & McClaine, A. W. (2017). Methods and Systems for Making Metal Hydride Slurries (Australian Patent Office Patent No. 2014223195). https://patents.google.com/patent/AU2014223195B2/en
10. Cherubini, F., Raugei, M., & Ulgiati, S. (2008). LCA of magnesium production. Resources, Conservation and Recycling, 52(8–9), 1093–1100. https://doi.org/10.1016/j.resconrec.2008.05.001
11. Ehrenberger, S., & Friedrich, H. E. (2013). Life-Cycle Assessment of the Recycling of Magnesium Vehicle Components. *JOM*, 65(10), 1303–1309. https://doi.org/10.1007/s11837-013-0703-
12. Ehrenberger, S. (2020). Carbon Footprint of Magnesium Production and its Use in Transport Applications. *International Magnesium Association*. https://cdn.ymaws.com/www.intlmag.org/resource/resmgr/sustainability/2020-LCA-Study-2021-02-09.pdf
13. Thayer, R. L., & Neelameggham, R. (2001). Improving the electrolytic process magnesium production. *JOM*, 53(8), 15–17. https://doi.org/10.1007/s11837-001-0128-2
14. Xie, K., Wang, S., & Zhu, H. (2018, May 16). Development and prospect of ecological magnesium industry in Qinghai Salt Lake. *International Magnesium Association*, 75th Annual Magnesium Conference, New Orleans, Louisiana, USA.
15. Fournier, J. (2021). A New Hydrometallurgical Process Combined With an Electrolytic Process for Magnesium Primary Production from Serpentine. In A. Luo, M. Pekguleryuz, S. Agnew, J. Allison, K. Kainer, E. Nyberg, W. Poole, K. Sadayappan, B. Williams, & S. Yue (Eds.), *Magnesium 2021* (pp. 3–11). Springer International Publishing. https://doi.org/10.1007/978-3-030-72432-0_1
16. Yerkes, L. A. (1947). Electrolytic Method for Producing Magnesium (U.S. Patent & Trademark Office Patent No. US 2,342,723). https://patents.google.com/patent/US2431723A/en
17. Lee, T.-H., Okabe, T. H., Lee, J.-Y., Kim, Y. M., & Kang, J. (2020). Molten Salt Electrolysis of Magnesium Oxide Using a Liquid–Metal Cathode for the Production of Magnesium Metal.

Metallurgical and Materials Transactions B, 51(6), 2993–3006. https://doi.org/10.1007/s11663-020-01976-9

18. Lee, T.-H., Okabe, T. H., Lee, J.-Y., Kim, Y. M., & Kang, J. (2021). Development of a novel electrolytic process for producing high-purity magnesium metal from magnesium oxide using a liquid tin cathode. *Journal of Magnesium and Alloys*, S2213956721000220. https://doi.org/10.1016/j.jma.2021.01.004
19. Rutherford, M., Telgerafchi, A. E., Espinosa, G., Powell, A. C., & Dussault, D. (2021). Low-Cost Magnesium Primary Production Using Gravity-Driven Multiple Effect Thermal System (G-METS) Distillation. *Magnesium 2021*, 139–144. https://doi.org/10.1007/978-3-030-65528-0_21
20. Moore, J. F., Hryn, J. N., Pellin, M. J., Calaway, W. F., & Watson, K. (2000). An Inert Metal Anode for Magnesium Electrowinning. In H. I. Kaplan, J. N. Hryn, & B. B. Clow (Eds.), *Magnesium Technology 2000* (pp. 21–26). John Wiley & Sons, Inc. https://doi.org/10.1002/9781118808962.ch4
21. Guan, X., Pal, U. B., & Powell, A. C. (2014). Energy-Efficient and Environmentally Friendly Solid Oxide Membrane Electrolysis Process for Magnesium Oxide Reduction: Experiment and Modeling. *Metallurgical and Materials Transactions E*, 1(2), 132–144. https://doi.org/10.1007/s40553-014-0013-x
22. Gratz, E. S., Guan, X., Milshtein, J. D., Pal, U. B., & Powell, A. C. (2014). Mitigating Electronic Current in Molten Flux for the Magnesium SOM Process. *Metallurgical and Materials Transactions B*, 45(4), 1325–1336. https://doi.org/10.1007/s11663-014-0060-9
23. Root, Tik. "Desalination Plants Produce More Waste Brine than Thought." National Geographic, 14 Jan. 2019, https://www.nationalgeographic.com/environment/article/desalination-plants-produce-twice-as-much-waste-brine-as-thought. Accessed 1 June 2021.
24. Doliente, S. S., Narayan, A., Tapia, J. F. D., Samsatli, N. J., Zhao, Y., & Samsatli, S. (2020). Bio-aviation Fuel: A Comprehensive Review and Analysis of the Supply Chain Components. *Frontiers in Energy Research*, 8, 110. https://doi.org/10.3389/fenrg.2020.00110